

High Performance 32nm Logic Technology Featuring 2nd Generation High-k + Metal Gate Transistors

P. Packan, S. Akbar, M. Armstrong, M. Brazier, H. Deshpande, K. Dev, G. Ding, T. Ghani, O. Golonzka, W. Han, J. He*, R. Heussner, R. James, J. Jopling, C. Kenyon, S-H. Lee, M. Liu, S. Lodha, B. Mattis, A. Murthy, L. Neiberg, J. Neiryneck, S. Pae*, C. Parker, L. Pipes, J. Sebastian, J. Seiple, B. Sell, S. Sivakumar, B. Song, A. St. Amour, K. Tone, T. Troeger, C. Weber**, K. Zhang, S. Natarajan
Logic Technology Development, * Quality and Reliability Engineering, ** TCAD, Intel Corporation.

Intel Corporation, RA3-353, 2501 NW 229th Ave., Hillsboro, OR 97124
Phone: (503) 613-8029; Fax: (503) 613-8950; e-mail: sanjay.natarajan@intel.com

Abstract:

A 32nm logic technology for high performance microprocessors is described. 2nd generation high-k + metal gate transistors provide record drive currents at the tightest gate pitch reported for any 32nm or 28nm logic technology. NMOS drive currents are 1.62mA/um Idsat and 0.231mA/um Idlin at 1.0V and 100nA/um Ioff. PMOS drive currents are 1.37mA/um Idsat and 0.240mA/um Idlin at 1.0V and 100nA/um Ioff. The impact of SRAM cell and array size on Vccmin is reported.

Technology Overview:

Continuing Moore's law to the 32nm technology node requires difficult trade-offs in gate length, S/D contact area and contact-to-gate margins. As dimensions are reduced, less area is available for introducing strain for mobility enhancement to improve device performance. To continue historical trends of both area and performance improvement requires novel solutions. In addition to intrinsic device performance improvement, the ability to operate at low Vcc is becoming even more critical for low power products. This paper presents a high performance, 112.5nm pitch high-k + metal gate strain enhanced technology that continues Moore's law to the 32nm technology node and enables low Vccmin operation.

Figure 1 shows the layer pitch, thickness and aspect ratio of Intel's 32nm technology. As the contacted gate pitch is reduced, trade-offs in gate length, S/D contact resistance and contact-to-gate margin determine performance. The reduction of area requires further improvements in strain technology for mobility enhancement. Figure 2 schematically demonstrates one of the scaling issues. For given short channel characteristics and constant Ioff, as gate lengths are decreased the threshold voltage must be increased. The improvement in drive current due to the shorter effective channel length is offset by the reduction in overdrive (Vg-Vt). For small channel lengths and low Vcc, the reduction in overdrive dominates and device drive currents are reduced. Figure 3 shows a 9% Idlin increase at fixed Ioff for a 36nm device with lower Vt compared to a 32nm device, demonstrating the trade-off between Vt and Lgate. This shows that even higher Id than reported in this paper could have been achieved with longer Lgate.

Transistors:

This 32nm technology uses 4th generation strained silicon and 2nd generation high-k and replacement metal gate flow [1-3]. Using a replacement metal gate flow enables stress enhancement techniques to be in place before removing the poly gate from the transistor. It has been shown that this can further enhance strain and is a key benefit of this flow [2, 4]. A cross section of the NMOS device is shown in Fig. 4. The introduction of raised source and drain regions enables reduced device resistance helping to mitigate the pitch scaling issues discussed above. The combination of 4th generation strained silicon and 2nd generation high-k + metal gate results in PMOS saturated (Vds=1.0V) and linear (Vds=0.05V) drive currents of 1.37mA/um and 0.240mA/um at 1.0V and 100nA/um Ioff (Figs. 5 and 6). These represent a 28% improvement in Idsat and a 35% improvement in Idlin over the 45nm technology and are the highest reported drive currents for any 32nm or 28nm technology. Furthermore, this is the first report of PMOS linear

drive current exceeding NMOS and is the result of 4 generations of PMOS strain engineering at Intel. NMOS saturated and linear drive currents are 1.62mA/um and 0.231mA/um at 1.0V and 100nA/um Ioff (Figs. 7 and 8). This is a 19% increase in Idsat and a 20% increase in Idlin over the 45nm technology. Device I-V and subthreshold characteristics are shown in Figs. 9 and 10. Subthreshold slopes are maintained at ~100mV/decade. Figure 11 shows good Vt roll-off and DIBL characteristics.

SRAM:

The ability to operate at low Vcc is critical for low power applications. Device variation plays a key role in determining the minimum operating voltage (Vccmin) for SRAM and RF circuits. Figures 12 and 13 show the 32nm technology continues the trend of 0.7x reduction in gate length variation and the magnitude of both systematic and random within wafer variation does not increase for the 32nm technology. In addition to device variation, cell size, array size and intrinsic distribution determine Vccmin for memory cells. Although it is relatively easy to produce a few small SRAM arrays that operate at low Vcc, the important goal is to produce large arrays that operate at low Vcc. Figure 14 shows the Vccmin distribution for a 3.25Mb array for cell sizes of 0.171um², 0.199um² and 0.256 um². As expected, the larger cell sizes support smaller Vccmin due to larger random variation for smaller devices. Vccmin can easily differ by 150 mV depending on the distribution percentage reported. Figure 15 shows the effect of array size on Vccmin for array sizes of 3.25Mb and 91Mb for a 0.199um² cell. The shift of 70mV is due to the statistics from the larger number of cells. The Vccmin data above is for active memory operation. For standby mode where the memory cell must only hold the bit, Vccmin can be more than 200mV lower (Fig. 16).

Cell size, Vccmin distribution, and array size must all be considered when comparing low voltage memory operation. Array density, which includes memory cells, sense amps and control circuitry, is another important SRAM metric to report. Figure 17 shows Intel's array density versus technology node, demonstrating the highest reported array density for a 32nm or 28nm technology of 4.2Mbit/mm².

Conclusion:

A high performance 32nm logic technology with 2nd generation high-k + metal gate transistors is presented. Record NMOS and PMOS drive currents are reported, along with the tightest contacted gate pitch for a 32nm or 28nm technology. Variation for the 32nm technology was shown to be the same as the 45nm technology. Excellent Vccmin and the highest reported SRAM array density for 32nm or 28nm technology was reported. Fully functional 32nm processors using this technology were demonstrated in systems in Jan 2009 and are on track for volume production in 2H 2009. This 32nm technology maintains the historical scaling trends of both area and performance and continues Moore's law.

References:

- [1] S.Natarajan et al., IEDM Tech. Dig., p. 941, (2008).
- [2] C.Auth et al., Symp. VLSI Dig., p 128, (2008).
- [3] K.Mistry et al., IEDM Tech. Dig., p.247, (2007).
- [4] J.Wang et al., VLSI Sym. Dig, p 46, (2007).

Layer	Pitch (nm)	Thick (nm)	Aspect Ratio
Isolation	140	200	--
Contacted Gate	112.5	35	--
Metal 1	112.5	95	1.7
Metal 2	112.5	95	1.7
Metal 3	112.5	95	1.7
Metal 4	168.8	151	1.8
Metal 5	225.0	204	1.8
Metal 6	337.6	303	1.8
Metal 7	450.1	388	1.7
Metal 8	566.5	504	1.8
Metal 9	19.4um	8um	1.5

Fig. 1 – Layer pitch, thickness and aspect ratio for Intel’s 32nm technology

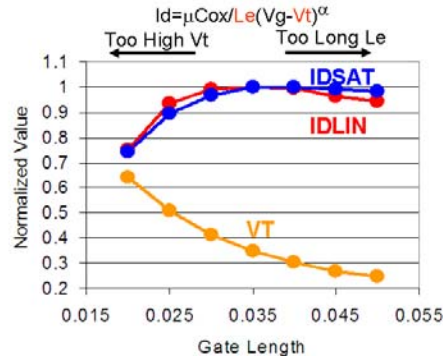


Fig. 2 - Normalized drive current and V_t vs. gate length. Both drive current and V_t are at constant I_{off} . At long gate length L_e dominates. At short gate length, $V_g - V_t$ dominates.

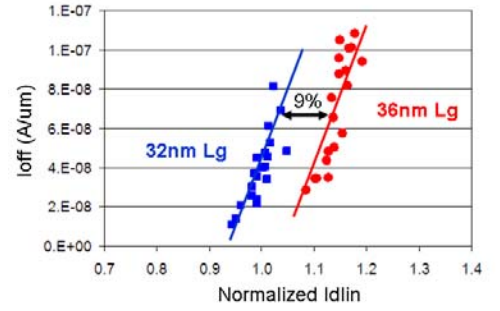


Fig. 3 – I_{off} vs. normalized I_{dlin} showing a 9% I_{dlin} increase for the 36nm device with lower V_t compared to the 32nm device.

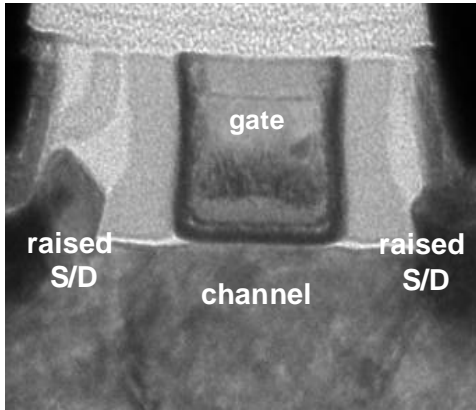


Fig. 4 – Cross section of NMOS device showing raised S/D regions for reduced parasitic resistance.

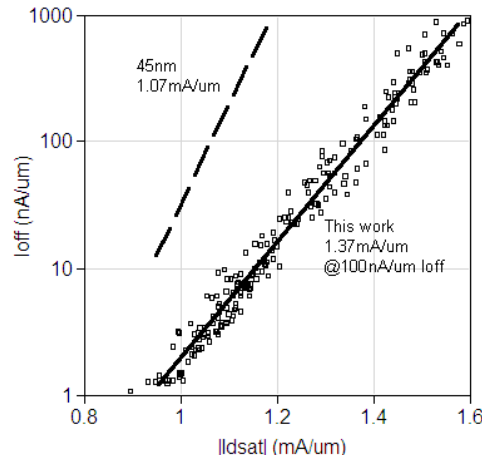


Fig. 5 – I_{off} vs. I_{dsat} for the PMOS device showing a 28% improvement over the 45nm technology ($V_{gs}=1.0V$, $V_{ds}=1.0V$)

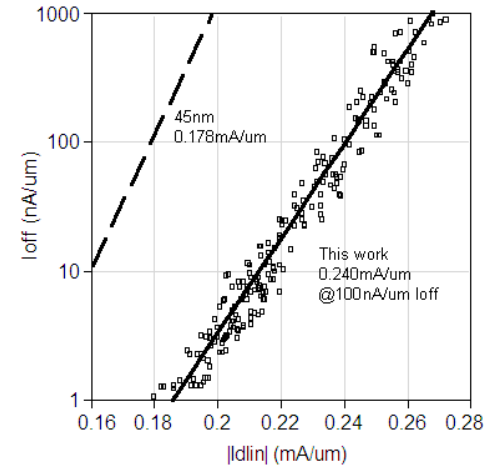


Fig. 6 – I_{off} vs. I_{dlin} for the PMOS device showing a 35% improvement over the 45nm technology ($V_{gs}=1.0V$, $V_{ds}=0.05V$)

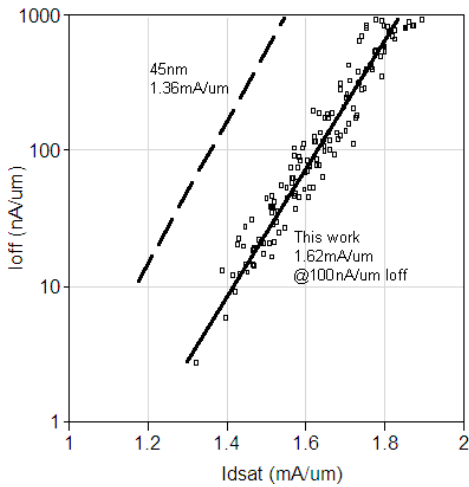


Fig. 7 – I_{off} vs. I_{dsat} for the NMOS device showing a 19% improvement over the 45nm technology ($V_{gs}=1.0V$, $V_{ds}=1.0V$)

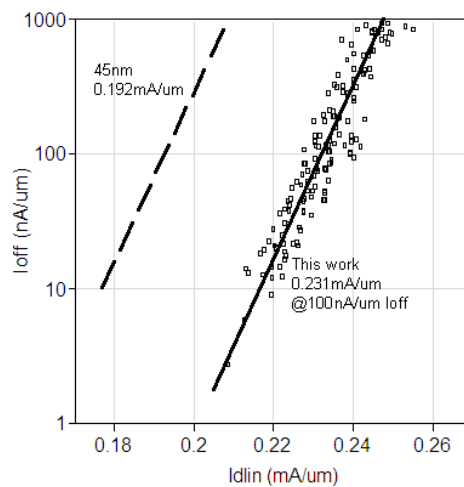


Fig. 8 – I_{off} vs. I_{dlin} for the NMOS device showing a 20% improvement over the 45nm technology ($V_{gs}=1.0V$, $V_{ds}=0.05V$)

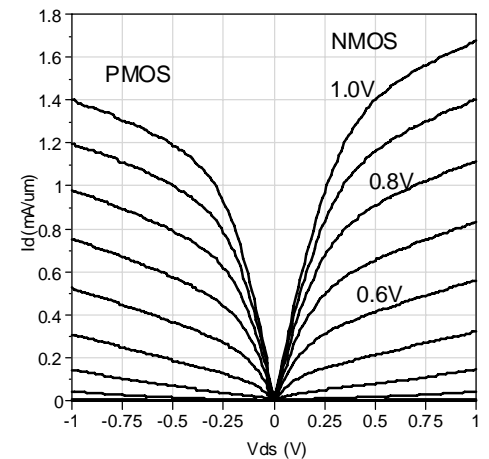


Fig. 9 – I-V characteristics for PMOS and NMOS devices.

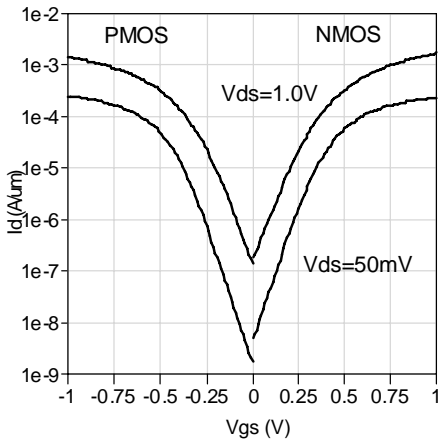


Fig. 10 – Subthreshold characteristics of PMOS and NMOS devices showing $<100mV/decade$ slope at $V_{ds}=1.0V$ & $50mV$.

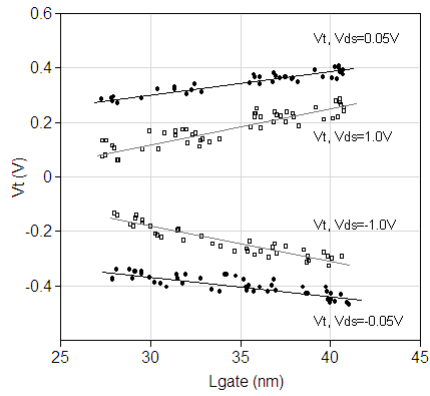


Fig. 11 – PMOS and NMOS V_t vs. gate length characteristics showing good V_t roll-off and DIBL characteristics.

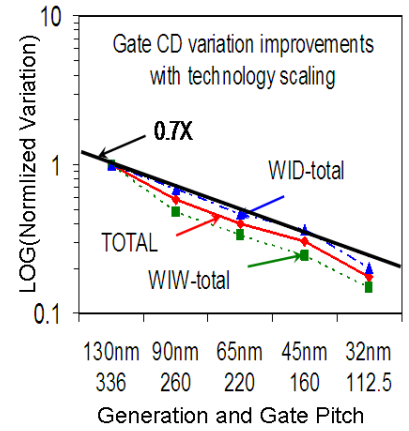


Fig. 12 – Gate length variation trend as a function of technology node showing a reduction in variation of 0.7x/generation.

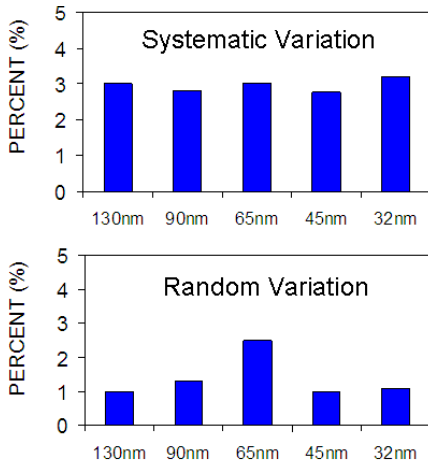


Fig. 13 – Within wafer systematic and random variation based on ring oscillator structures vs. technology node. The 32nm node has similar variation compared to the 45nm node.

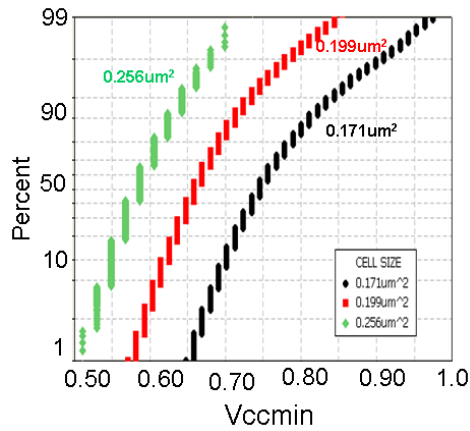


Fig. 14 – V_{ccmin} distribution for a 3.25Mb array for cell sizes of $0.171\mu m^2$, $0.199\mu m^2$ and $0.256\mu m^2$. As expected, the larger cell sizes support smaller V_{ccmin} .

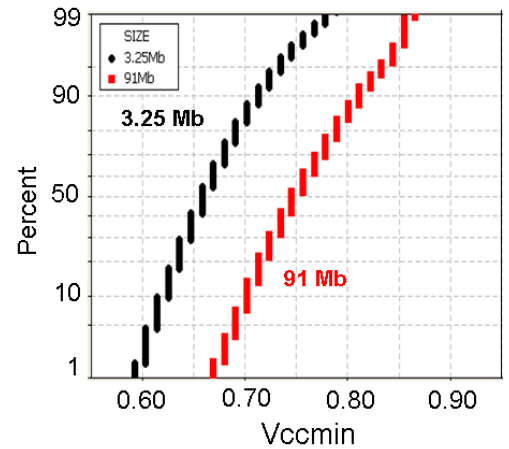


Fig. 15 – V_{ccmin} distribution for array sizes of 3.25Mb and 91Mb for the $0.199\mu m^2$ cell. The shift of 70mV is due to the statistics from the larger number of cells.

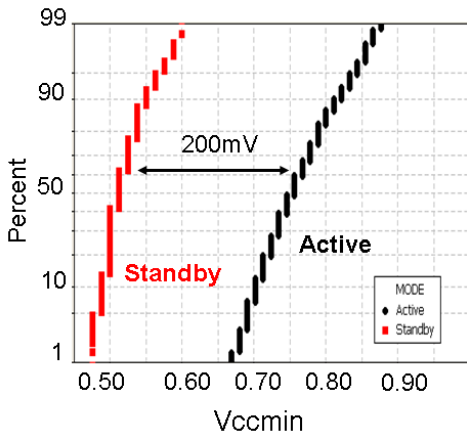


Fig. 16 – V_{ccmin} distribution comparing active and standby modes. Standby mode can have a 200mV lower V_{ccmin} .

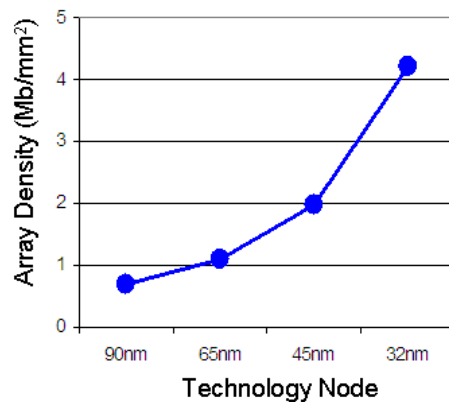


Fig. 17 – Intel's array density vs. technology node demonstrating excellent scaling and the highest reported array density for the 32nm node.